LANGMUIR Article
Cite This: Langmuir 2018, 34, 10764−10773
pubs.acs.org/Langmuir

# Membrane Reconstitution of Monoamine Oxidase Enzymes on Supported Lipid Bilayers

Liulin Wang,[†,‡,⊥] Kabir H. Biswas,[‡,⊥] Bo Kyeong Yoon,[‡] Lisa M. Kawakami,[‡] Soohyun Park,[‡] Jay T. Groves,[‡,§] Lin Li,[*,†] Wei Huang,[†] and Nam-Joon Cho[*,‡,∥]

[†]Key Laboratory of Flexible Electronics (KLOFE) & Institute of Advanced Materials (IAM), Jiangsu National Synergetic Innovation Center for Advanced Materials (SICAM), Nanjing Tech University (NanjingTech), Nanjing 211816, China
[‡]School of Materials Science and Engineering, Nanyang Technological University, Singapore 639798, Singapore
[§]Department of Chemistry, University of California, Berkeley, Berkeley, California 94720, United States of America
[∥]School of Chemical and Biomedical Engineering, Nanyang Technological University, Singapore 637459, Singapore

Supporting Information

**ABSTRACT:** Monoamine oxidase A and B (MAO-A and B) are mitochondrial outer membrane enzymes that are implicated in a number of human diseases, and the pharmacological inhibition of these enzymes is a promising therapeutic strategy to alleviate disease symptoms. It has been suggested that optimal levels of enzymatic activity occur in the membrane-associated state, although details of the membrane association process remain to be understood. Herein, we have developed a supported lipid bilayer platform to study MAO-A and B binding and evaluate the effects of known pharmacological inhibitors on the membrane association process. By utilizing the quartz crystal microbalance-dissipation (QCM-D) technique, it was determined that both MAOs exhibit tight binding to negatively and positively charged bilayers with distinct concentration-dependent binding profiles while only transiently binding to neutral bilayers. Importantly, in the presence of known inhibitors, the MAOs showed increased binding to negatively charged bilayers, although there was no effect of inhibitor treatment on binding to positively charged bilayers. Taken together, our findings establish that the membrane association of MAOs is highly dependent on membrane surface charge, and we outline an experimental platform to support the in vitro reconstitution of monoamine oxidases on synthetic membranes, including the evaluation of pharmacological drug candidates.

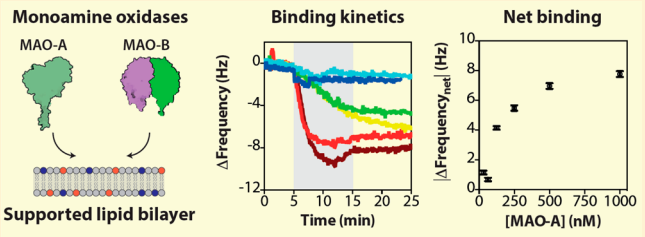


## INTRODUCTION

Monoamine oxidases (MAOs) are monotopic, outer mitochondrial membrane proteins that regulate the concentration of monoamine neurotransmitters such as dopamine, serotonin, norepinephrine, and phenylethylamine as well as other amines by catalyzing their oxidative deamination with the release of hydrogen peroxide as a byproduct.[1−4] The enzymes are expressed from different genes[4] as two isoforms, MAO-A and MAO-B, and are involved in central nervous system development.[5] Mutations in MAO-A cause Brunner syndrome, which is characterized by impulsive aggressiveness, mild mental retardation,[6−8] and behavioral aggression,[9] while the deletion of MAO-B is associated with atypical Norrie's disease, which is characterized by blindness and impaired hearing (*10*, *11*). Furthermore, the enzymes have been implicated in a number of diseases such as neurodegenerative disorders including Parkinson's disease and Alzheimer's disease,[12,13] cardiovascular diseases,[14] and certain cancers[15,16] and have been targeted with pharmacological inhibitors in some cases (*17*−*19*). Additionally, tracer compounds have been developed on the basis of their enzymatic activity for the in vivo monitoring of pathological conditions.[20] From a protein engineering perspective, enzymes within this class have also been modified to perform novel chemical transformations such as the deracemization of racemic chiral amines,[21] thus illustrating their utility across the pharmaceutical and biotechnology industries.

A key feature of MAO-A and MAO-B is that their localization to the mitochondrial outer membrane is important for their function.[22,23] In fact, they are tightly bound to the membrane and require detergents for extraction from the mitochondrial outer membrane. Structural studies have shed some light on the possible mechanism of their localization.[24−27] Both MAO-A and MAO-B contain a globular domain at the N-terminus and a single transmembrane domain at the C-terminus, the latter of which is thought to be important for membrane insertion in a perpendicular manner. However, the two domains are not independent of one another because the C-terminal transmembrane regions of MAO-A and MAO-B cannot be interchanged,[28] despite sharing relatively high sequence identity. This finding indicates that the interaction

Received: April 24, 2018
Revised: July 24, 2018
Published: July 26, 2018

between the two domains is a key determinant of their enzymatic activity. Furthermore, the transmembrane domain is not the sole membrane interaction module in these proteins since truncation or complete deletion mutation of this region does not result in a complete loss of membrane localization.[29] Structural analysis has indicated the possible interactions of certain amino acid residues in the protein with the mitochondrial outer membrane[30] while molecular dynamics simulations have revealed the possibility of several hydrogen bonds forming between proteins and phospholipid headgroups.[31] Aside from providing a two-dimensional space for the localization of proteins, the membrane surface has also been suggested to facilitate the electrostatic channeling of the substrates into the catalytic site since the substrate entrance site is predicted to be close to the membrane surface.[24−27]

Because the membrane association of MAO-A and MAO-B is functionally critical, numerous efforts have been directed toward the in vitro reconstitution of these enzymes in a membranelike environment. Initially, a purified phospholipid such as phosphatidylinositol or phosphatidylserine was added to membrane-free preparations of the enzymes.[23,32] These studies showed the restoration of the catalytic activity of the enzymes with marked improvement over the membrane-free versions, suggesting a direct interaction between proteins and phospholipids. In another direction, attempts have been made to insert in vitro translated MAO-A[33] and MAO-B[34,35] into isolated mitochondrial outer membrane fractions. These experiments suggested that the membrane insertion of the proteins is an active process requiring ATP and ubiquitin, and the binding of inhibitors may inhibit membrane insertion. The isolated mitochondrial outer membrane fractions used in these early studies had complex structures, including the presence of membrane domains and other membrane-bound proteins, thus complicating the reconstitution experiments. Hence, there is a need to reconstitute MAO-A and MAO-B enzymes in much simpler, synthetic membranes. To this end, Cruz and Edmondson[36] have used membrane nanodiscs, which are small phospholipid bilayers fenced by an engineered scaffold membrane protein, to prepare membrane-bound MAO-A for biochemical characterization of the protein in a membranous environment. It was identified that membrane-bound MAO-A has ∼3-fold higher catalytic activity and inhibitor affinity compared to that of the detergent-solubilized protein. Hence, successful membrane reconstitution in simplified model systems establishes a premise for the restoring the function of MAO-A and MAO-B enzymes, and interfacing these proteins with surface-engineered model membrane platforms would further enhance the experimental capability to characterize the structure and function of membrane-associated enzymes.

Here, we report that MAO-A and MAO-B proteins could be successfully reconstituted in a supported lipid bilayer platform that is compatible with surface-sensitive measurement techniques. Following this approach, quartz crystal microbalance with dissipation (QCM-D) monitoring[37−39] experiments revealed the preferential binding of the proteins to charged bilayers while they interacted transiently with the neutral bilayer. We also demonstrate that the binding of inhibitors, clorgyline and rasagiline, to MAO-A and MAO-B, respectively, specifically enhances their binding to negatively charged bilayers. Taken together, this study describes the establishment of an in vitro membrane-based platform for MAO-A and MAO-B. We envision that the technology presented herein will find broad application in the further study of the mechanism of membrane interaction of MAO-A and MAO-B as well as in developing potential therapeutic compounds with desired molecular interaction profiles.

## MATERIALS AND METHODS

**Reagents.** 1,2-Dioleoyl-*sn*-glycero-3-phosphocholine (DOPC), 1,2-dioleoyl-*sn*-glycero-3-ethylphosphocholine (DOEPC), and 1,2-dioleoyl-*sn*-glycero-3-phospho-L-serine (DOPS) were obtained from Avanti Polar Lipids (Alabaster, AL). The lipid chloroform solutions were stored at −20 °C. MAO-A (catalog no. M7316-1VL) and MAO-B (catalog no. M7441-1VL) enzymes were obtained from Sigma-Aldrich (St. Louis, MO), and 5 mg/mL stock aliquots of each enzyme were stored at −70 °C in potassium phosphate buffer solution (pH 7.4, 0.25 M sucrose, 0.1 mM EDTA, and 5% glycerol) until use. The degree of enzymatic activity was measured by monitoring the rate of kynuramine deamination, and the experimentally determined activities of MAO-A and MAO-B enzymes were ≥10 and ≥1 units/mg protein, respectively, where 1 unit is defined as the amount needed to deaminate 1 nanomole of kynuramine per minute at pH 7.4 at 37 °C. Clorgyline (MAO-A inhibitor), and rasagiline (MAO-B inhibitor) were also procured from Sigma-Aldrich. Inhibitors in powder form were stored at 4 °C until use and dissolved in DMSO at a stock concentration of 50 μM before use. All experiments were performed in an aqueous buffer containing 10 mM Tris buffer solution (pH 7.5) and 150 mM NaCl. All other reagents were obtained from Sigma-Aldrich. Milli-Q-water (>18 MΩ·cm) (Millipore, Billerica, MA) was used in all experiments.

**Supported Lipid Bilayer Preparation.** All SLBs used in the study were assembled on silicon dioxide crystals using the solvent-assisted lipid bilayer (SALB) technique.[40] It is an alternate method for the fabrication of SLBs that does not require the preparation of lipid vesicles. DOPC, DOEPC, and DOPS lipids in chloroform (5 mg/mL) were mixed in the desired lipid molar ratio in glass tubes. Chloroform was then evaporated from the glass tube under constant rotation using a gentle flow of nitrogen. Lipid mixtures were then diluted at a concentration of 0.4 mg/mL by dissolution in a 1:1 (volume/volume) mixture of isopropanol (IPA) and water. To assemble the bilayer on the silicon dioxide substrate in the QCM-D setup, an aqueous buffer was injected into the QCM-D measurement chamber for 15 min to stabilize frequency and energy dissipation signals. The system was further stabilized in IPA for 15 min. Following this, lipid mixtures in IPA/water injected into the system and the lipid molecules were allowed to interact with the substrate for 10 min. Finally, lipid mixtures in IPA/water were replaced with the aqueous buffer to trigger the formation of SLBs with $\Delta f$ and $\Delta D$ shifts of $-25 \pm 3$ Hz and less than $(0.5 \pm 0.3) \times 10^{-6}$, respectively, indicating the successful assembly of SLBs.[37]

**Protein−Bilayer Interaction.** MAO-A and MAO-B were dissolved in potassium phosphate buffer solution (pH 7.4, 0.25 M sucrose, 0.1 mM EDTA, and 5% glycerol) at 5 mg/mL concentration. An aliquot from the stock compound was diluted with Tris buffer to obtain the desired test concentration. Stock solutions of clorgyline and rasagiline were prepared by dissolving the weighed compounds in DMSO to a final concentration of 50 μM. The stock compound solution was further diluted with Tris buffer to the desired test concentration. In incubation experiment of MAOs (MAO-A and MAO-B) and their inhibitors, the samples with varying MAO/inhibitor molar ratios were incubated at 4 °C for an hour before they were injected. MAO-A and MAO-B were stored at −70 °C, and dissolved clorgyline and rasagiline solutions were stored at 4 °C.

**Quartz Crystal Microbalance-Dissipation (QCM-D) Monitoring.** A Q-Sense E4 instrument (Q-Sense AB, Gothenburg, Sweden) was employed to monitor the interaction between the proteins and supported lipid bilayers (SLBs). The QCM-D technique detects shifts in the resonance frequency ($\Delta f$) and energy dissipation ($\Delta D$) that relate to the acoustic mass and viscoelastic properties of the test samples, respectively.[41] The sensor chip had a fundamental frequency of 5 MHz and a sputter-coated, 50-nm-thick layer of silicon dioxide (model no. QSX 303, Q-Sense AB). The measurement data was



DOI: 10.1021/acs.langmuir.8b01348
*Langmuir* 2018, 34, 10764−10773

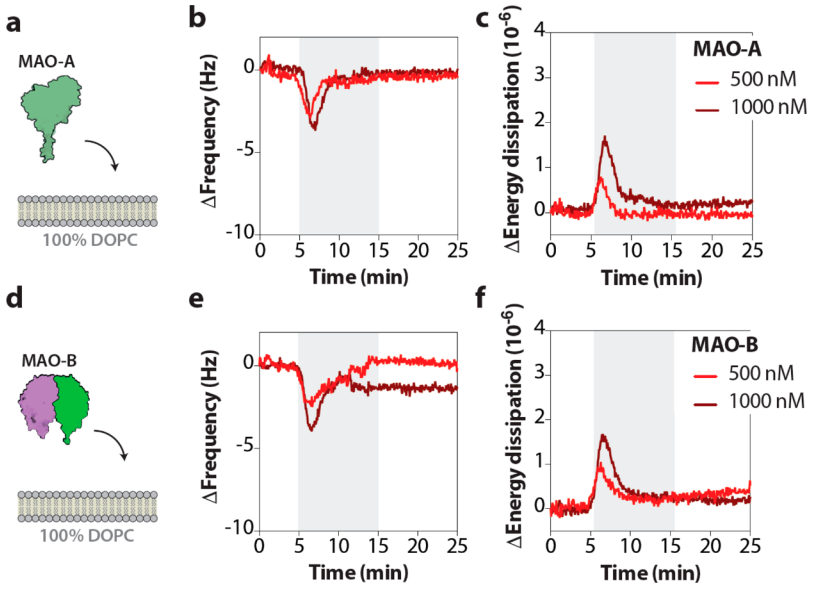


**Figure 1.** Transient interaction of MAO-A and MOA-B with neutral DOPC bilayers. (a, d) Schematics showing MAO-A (a) and MAO-B (d) incubated with the DOPC bilayer. (b, e) Temporal shifts in frequency observed with either 500 or 1000 nM MAO-A (b) or MAO-B (e). (c, f) Temporal shifts in energy dissipation observed with either 500 or 1000 nM MAO-A (c) or MAO-B (f). The gray area in the graphs corresponds to the duration of the protein injection.

collected at the $n$ = 3−11 odd overtones using the QSoft software program (Q-Sense AB). All presented data was collected at the fifth overtone. Data processing was performed in the QTools (Q-Sense AB) and OriginPro 8.6 (OriginLab, Northampton, MA) software packages.

Prior to measurements, QCM-D substrates were rinsed multiple times with 1% sodium dodecyl sulfate (SDS), water, and ethanol, dried with nitrogen gas, and subjected to oxygen plasma treatment for 1 min with an expanded plasma cleaner (model no. PDC-002, Harrick Plasma, Ithaca, NY). SLBs were assembled on the silicon dioxide substrates as described above.[40] During the experiments, the temperature of the flow cell was maintained at 24.0 ± 0.5 °C. All samples were injected at a flow rate of 50 μL/min using a peristaltic pump (Ismatec RegloDigital) for 10 min and were incubated for 15 min in the measurement chambers. Net frequency and energy dissipation shifts were calculated by determining the average values before sample injection and after equilibration in each experiment.

## RESULTS AND DISCUSSION

**Interaction of MAO-A and MAO-B with Neutral Bilayers.** We aimed to investigate the interaction of monoamine oxidases with phospholipid membranes and the impact of the membrane surface charge on the interaction. For this, we developed an in vitro reconstitution system wherein the proteins were allowed to interact with synthetic SLBs prepared with either DOPC alone or in combination with charged lipids (DOPS for negatively charged and DOEPC for positively charged bilayers) (Figure S1). The neutral and charged lipid molecules have the same hydrophobic tail while they differ in the headgroups. The interaction of the proteins with bilayers was monitored in real time by QCM-D, which is a label-free, acoustic-based technique that provides information on the binding of materials to a surface. Specifically, the binding of any material to the quartz crystal results in a change in its characteristic frequency, which is related to the mass of the bound material, as well as a change in its energy dissipation, which provides information on the viscoelastic properties of the bound material.[37,39,42] The quartz crystals were coated with a thin layer of silicon dioxide for the purpose of assembling SLBs. All SLBs used in the study were assembled using the recently developed solvent-assisted lipid bilayer (SALB) formation method.[40] The key advantage of using the SALB method is that it enables the fabrication of bilayers with negatively charged lipid molecules under neutral pH conditions, which is not possible with the traditional vesicle fusion method of membrane assembly.[43,44] The quality of all assembled bilayers used in the study was ascertained from the magnitude of shifts in frequency and energy dissipation. For instance, the neutral DOPC bilayer had a frequency decrease of −25 ± 0.2 Hz and an energy dissipation of $(0.5 \pm 0.3) \times 10^{-6}$, respectively, values which agree well with previous reports describing SLB assembly.[37,40] Furthermore, all experiments were performed using recombinant microsomal MAO-A and MAO-B proteins (Figure S2), which have been previously utilized for inhibitor[45,46] and mutant screening.[47]

The incubation of MAO-A with the zwitterionic, neutral DOPC bilayer (Figure 1a) at a concentration of either 500 or 1000 nM resulted in an initial decrease in the frequency (−2.8 and −3.3 Hz, respectively) with a concomitant increase in energy dissipation ($0.8 \times 10^{-6}$ and $1.6 \times 10^{-6}$, respectively) (Figure 1b,c). The magnitude of the initial frequency decrease was proportional to the protein concentration. However, the initial frequency decreases recovered close to the initial values with time. Similar initial decreases in frequency followed by a phase of recovery were observed with 500 or 1000 nM MAO-B (Figure 1d−f). These results suggest that both MAO-A and MAO-B interact transiently with the neutral DOPC bilayers, perhaps through electrostatic interaction with the zwitterionic headgroup of DOPC molecules,[48] and may require additional factors for stable binding.

**Interaction of MAO-A and MAO-B with Negatively Charged Bilayers.** Incubation of MAO-A with negatively charged DOPS-containing bilayers (30:70 DOPS:DOPC) (Figure 2a) resulted in a concentration-dependent initial frequency decreases and concomitant changes in energy dissipation (Figure 2b,c). The magnitude of the initial frequency decreases observed with 500 and 1000 nM MAO-A (−7.7 and −9.8 Hz, respectively) were greater compared to those



DOI: 10.1021/acs.langmuir.8b01348
Langmuir 2018, 34, 10764−10773

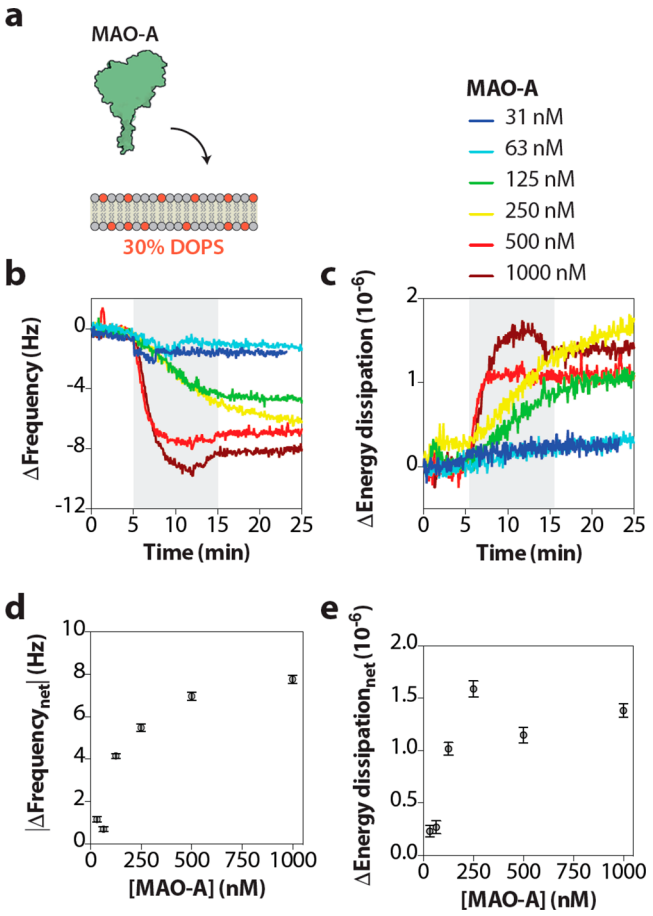


**Figure 2.** Stable interaction of MAO-A with negatively charged DOPC/DOPS bilayers. (a) Schematic of MAO-A incubated with a 30 mol % DOPS bilayer. (b, c) Temporal shifts in frequency (b) and energy dissipation (c) observed with the indicated concentrations of MAO-A. The gray area in the graphs corresponds to the duration of protein injection. (d, e) Net changes in frequency (d) and energy dissipation (e) plotted as a function of MAO-A concentration. Data presented are the mean ± SD.

observed on neutral DOPC bilayers, suggesting an enhanced interaction of the protein with the negatively charged bilayers. More importantly, the initial frequency decreases were stable after incubation (Figure 2b), suggesting that MAO-A is stably bound to the bilayer perhaps due to its insertion into the bilayer. Another key observation is that the net frequency changes determined at different concentrations saturate after 500 nM MAO-A with a magnitude of ∼7.0 Hz (Figure 2d), suggesting that either the negatively charged lipid molecules in the bilayer or the protein molecules are limiting, and thus no further binding of MAO-A is observed. A closer inspection of MAO-A binding kinetics at 1000 nM (Figure 2b) showed that the initial frequency decrease was greater than the final frequency decrease, suggesting that the number of protein molecules transiently interacting with the bilayer was greater than the number of proteins that could be stably bound to the bilayer. This leads to the idea that the stable binding of the protein is a two-step process in which the protein initially interacts with the bilayer in a transient manner irrespective of the membrane surface charge, followed by a stable insertion of the protein into the bilayer that is observed with the negatively charged bilayer. A similar two-step binding process has been reported for bee venom phospholipase $A_2$ on SLB platforms as well.[49]

The incubation of MAO-B with the negatively charged bilayer (Figure 3a) also resulted in concentration-dependent,

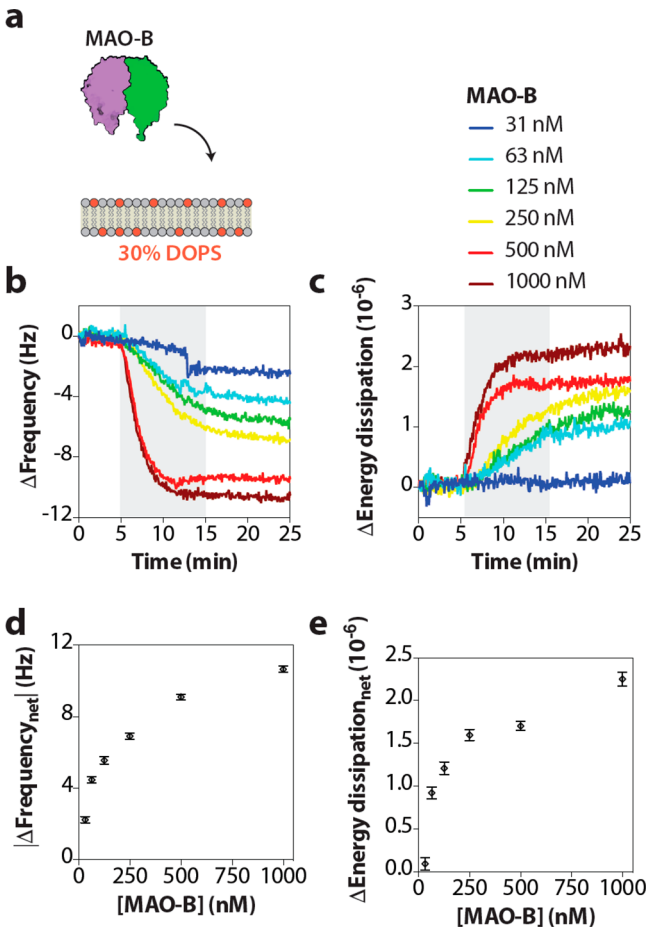


**Figure 3.** Stable interaction of MAO-B with negatively charged DOPC/DOPS bilayers. (a) Schematic of MAO-B incubated with a 30 mol % DOPS bilayer. (b, c) Temporal shifts in frequency (b) and energy dissipation (c) observed with the indicated concentrations of MAO-B. The gray area in the graphs corresponds to the duration of protein injection. (d, e) Net changes in frequency (d) and energy dissipation (e) plotted as a function of MAO-B concentration. Data presented are the mean ± SD.

stable frequency decreases with concomitant increases in energy dissipation (Figure 3b,c), as seen with MAO-A (Figure 2). The magnitudes of frequency decrease appeared to saturate at a concentration of 250 nM with a net frequency decrease of ∼10 Hz reflecting a greater mass of MAO-B bound to the bilayer in comparison to MOA-A (Figure S3a). This difference in the bilayer-bound masses of MAO-A and MAO-B is not due to a difference in the molecular weight of the proteins (molecular weight of MAO-A and MAO-B are 59.7 and 58.8 kDa, respectively). Instead, it could arise from a difference in their oligomeric state: while human MAO-A is a monomer,[26,27] MAO-B is a dimer[50] and therefore the binding of one monomer of MAO-B will cause the binding of the other monomer. Indeed, a small but significant difference could be observed in the slope of energy dissipation vs frequency shift plots of MAO-A and MAO-B at a concentration of 1000 nM (Figure S3b), suggesting a difference in the mechanism of their interaction with the negatively charged bilayers. Additionally, this could be due to a difference in the distribution of the charged amino acid



DOI: 10.1021/acs.langmuir.8b01348
Langmuir 2018, 34, 10764−10773

residues on the surface of these proteins. Importantly, the ability of both MAO-A and MAO-B to discriminate between the neutral DOPC and the negatively charged DOPS bilayers suggests that the proteins are functional and are likely present in their native conformation. We note that the activity of both MAO-A and MAO-B has been shown to be positively impacted by negatively charged membranes;[51] therefore, the results presented here provide a biochemical basis for this mode of their regulation.

**Interaction of MAO-A and MAO-B with Positively Charged Bilayers.** Having shown that the monoamine oxidases can bind to negatively charged, but not neutral, bilayers, we then investigated their interaction with the positively charged DOEPC-containing bilayers (30:70 DOEPC/DOPC). The incubation of MAO-A with the positively charged bilayer (Figure 4a) resulted in a concentration-dependent decrease in the frequency and a concomitant increase in the dissipation energy (Figure 4b,c). Importantly, the net frequency decreases for equivalent concentrations of MAO-A were much higher on the positively charged bilayer than on the negatively charged bilayer, indicating enhanced binding of the protein (Figure 4d).

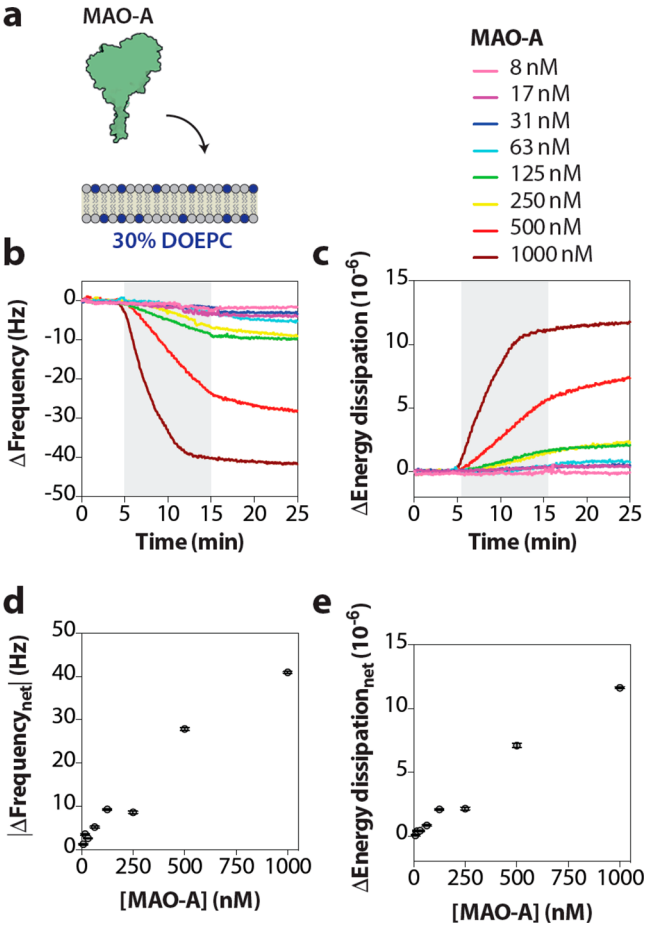


**Figure 4.** Stable interaction of MAO-A with positively charged DOPC/DOEPC bilayers. (a) Schematic of MAO-A incubated with a 30 mol % DOEPC bilayer. (b, c) Temporal shifts in frequency (b) and energy dissipation (c) observed with the indicated concentrations of MAO-A. The gray area in the graphs corresponds to the duration of protein injection. (d, e) Net changes in frequency (d) and energy dissipation (e) plotted as a function of MAO-A concentration. Data presented are the mean ± SD.

Furthermore, no clear saturation in the binding could be observed until a concentration of 1000 nM was reached, suggesting that the positively charged DOEPC molecules are much more effective than the negatively charged DOPS molecules in enabling the stable insertion of the protein into SLBs. A fairly similar pattern of binding was observed for MAO-B on these bilayers, except that the net frequency changes were greater for MAO-B than for MAO-A at each concentration tested (Figure 5a–e). The later observation is similar to that with the negatively charged bilayer described above. An increased binding of the proteins to the positively charged bilayers may point to a differential distribution of the

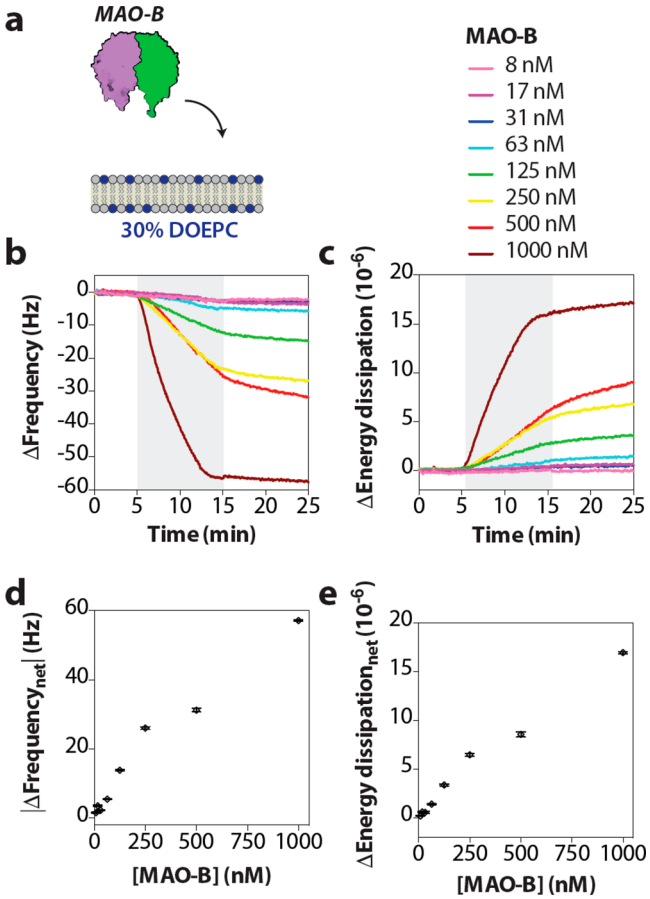


**Figure 5.** Stable interaction of MAO-B with positively charged DOPC/DOEPC bilayers. (a) Schematic of MAO-B incubated with a 30 mol % DOEPC bilayer. (b, c) Temporal shifts in frequency (b) and energy dissipation (c) observed with the indicated concentrations of MAO-B. The gray area in the graphs corresponds to the duration of protein injection. (d, e) Net changes in frequency (d) and energy dissipation (e) plotted as a function of MAO-B concentration. Data presented are the mean ± SD.

positively and negatively charged amino acid residues on the surface of the proteins. An analysis of the charged amino acid distribution on the surface of MAO-B (PDB ID 1GOS),[24] however, showed no substantial differences (Figure S4a). Furthermore, predicted isoelectric points (pI's) of 7.9 and 7.2 for MAO-A and MAO-B, respectively, also rule out the possibility of a general prevalence of charged amino acid residues on the protein surfaces at the experimental pH of 7.5. Another possibility that may explain the differences in their binding to the charged bilayers is the post-translational



DOI: 10.1021/acs.langmuir.8b01348
Langmuir 2018, 34, 10764–10773

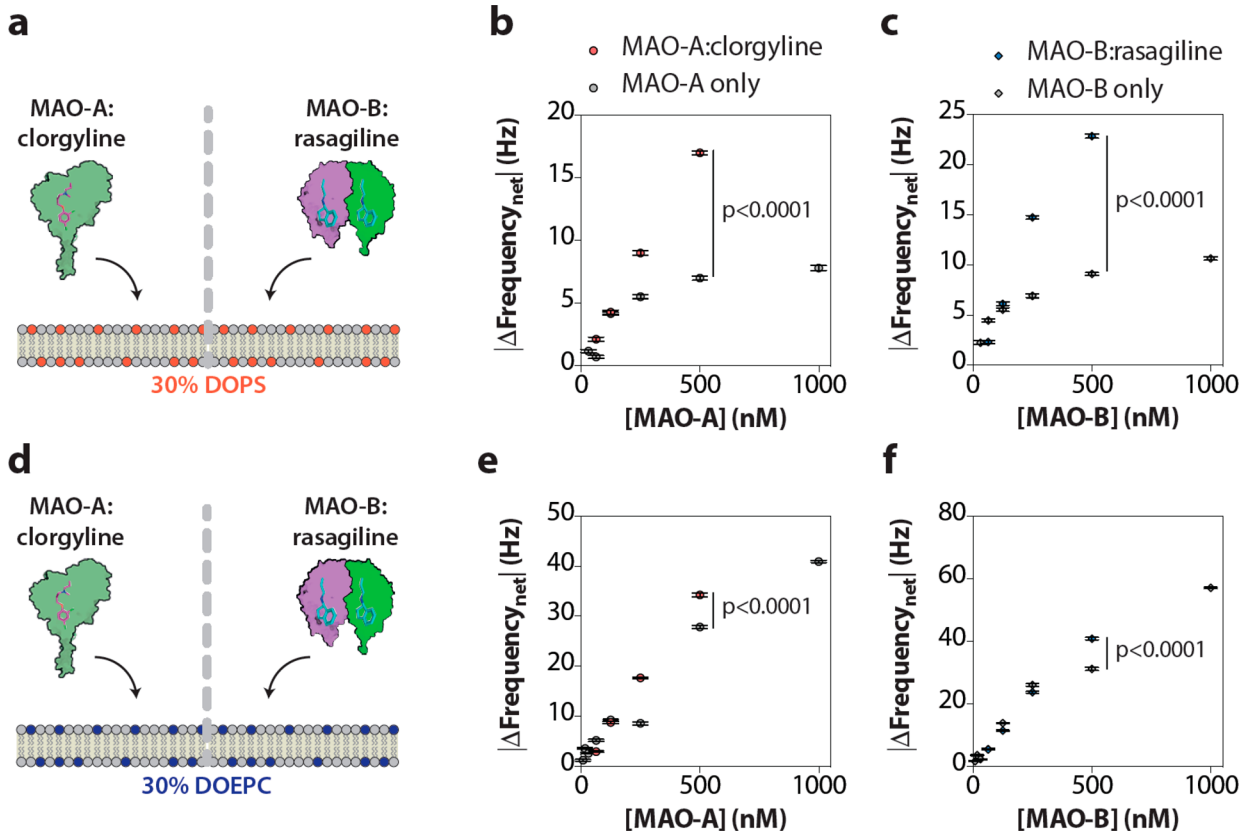


**Figure 6.** Enhanced interaction of inhibitor-bound MAO-A and MAO-B with a negatively charged bilayer. (a, d) Schematics of MAO-A/clorgyline and MAO-B/rasagiline incubated with either 30% DOPS (a) or DOEPC (d) bilayers. (b, c) Net frequency changes measured on the incubation of MAO-A/clorgyline (b) or MAO-B/rasagiline (c) with a 30% DOPS bilayer. (e, f) Net frequency changes measured on incubation of MAO-A/clorgyline (e) or MAO-B/rasagiline (f) with 30% DOEPC bilayers. Data presented are mean ± SD, and the *p* values shown in the graphs were obtained from an unpaired *t*-test analysis.

modification of the proteins such as phosphorylation, which imparts negative charges, often on the surface, to the protein and thus could increase the binding of the protein to the positively charged bilayers.[52,53] We note that the binding of the enzymes with the positively charged bilayers generally resulted in larger changes in the energy dissipation of the system in comparison to that of the negatively charged bilayers (Figures 2c,e, 3c,e, 4c,e, 5c,e, and S3a,b,c,d), indicating a higher viscoelastic nature of the bound enzyme molecules. This response and the difference in the bound mass clearly establish that the enzymes bind to the negatively charged bilayer via binding to DOPS lipid molecules, leading to a tighter association of the enzymes to the bilayer while they bind to the positively charged bilayer via specific interactions with a few DOEPC lipid molecules, leading to a flexible association of the enzymes with the positively charged bilayers.

**Irreversible Inhibitors Enhance the Binding of MAO-A and MAO-B Specifically to Negatively Charged Bilayers.** The establishment of an in vitro membrane reconstituted system described above encouraged us to investigate the effect of inhibitor binding on the membrane interaction of MAO-A and MAO-B since previous reports have suggested an inhibition of membrane insertion of the proteins upon inhibitor binding.[33] Specifically, we determined the binding kinetics of MAO-A and MAO-B complexed with clorgyline and rasagiline, respectively, with either negatively or positively charged bilayers. To do this, the proteins were preincubated with their respective inhibitors in a molar ratio of 1:2 (protein/inhibitor) for 1 h at 4 °C, following which the protein/inhibitor complexes were injected into the system and binding was monitored using QCM-D. Both clorgyline and rasagiline are high-affinity ($IC_{50}$ values of 1.2 and 14 nM for MAO-A and MAO-B, respectively),[54,55] irreversible inhibitors that act by forming adducts in a 1:1 protein/inhibitor ratio (in the case of MAO-B, each monomer binds one rasagiline molecule); therefore, we assume that all protein molecules are bound to their respective inhibitor molecules when incubated with excess inhibitors (molar ratio of 1:2) for a prolonged period of 1 h. Thus, the frequency changes observed in the QCM-D monitoring primarily arise from the binding of protein/inhibitor complexes to the bilayers. To determine the contributions of the unbound inhibitor molecules to the frequency and energy dissipation of the system, we incubated free clorgyline and rasagiline at a concentration of 500 nM with charged bilayers (Figure S5a,d). We chose this concentration by assuming that the maximum concentration of free inhibitor molecules in the experiment with protein/inhibitor complexes will be 500 nM. The incubation of both clorgyline and rasagiline with the negatively charged DOPS-containing bilayer resulted in small but significant changes in the frequency (Figure S5b,g) and energy dissipation (Figure S5c,h), suggesting a stable interaction of the inhibitors with these bilayers. On the other hand, the incubation of the inhibitors with the positively charged DOEPC-containing bilayers resulted in transient changes in the frequency and energy dissipation of the system (Figure S5e,h).

The incubation of MAO-A/clorgyline and MAO-B/rasagiline complexes with the negatively charged, DOPS-containing



DOI: 10.1021/acs.langmuir.8b01348
*Langmuir* 2018, 34, 10764−10773

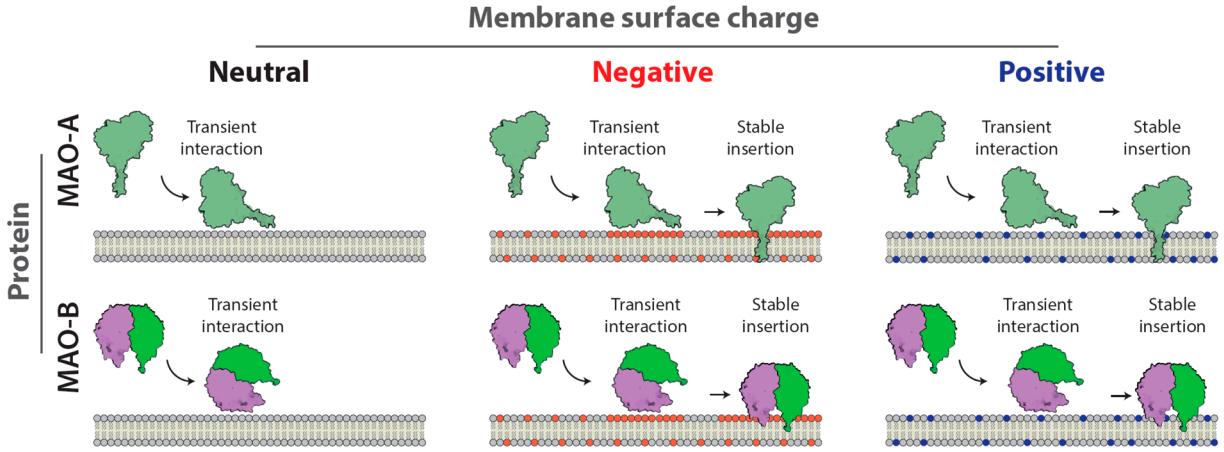


**Figure 7.** Proposed mechanism of MAO-A and MAO-B interaction with bilayers. A schematic representing the mechanism of interaction of MAO-A and MAO-B with SLBs. The proteins interact transiently with the neutral DOPC bilayers. The transient interaction leads to their stable insertion into the bilayers in the presence of either negatively or positively charged lipid molecules.

bilayer (Figure 6a) resulted in concentration-dependent decreases in the frequency (Figures S6b, S7b, and 6b,c) and increases in the energy dissipation (Figures S6c,d and S7c,d). However, the magnitude of frequency changes observed with the protein/inhibitor complexes increased linearly with increasing concentration of the protein/inhibitor complex up to 500 nM, an observation which is significantly different from the saturation seen with the apo proteins (Figures 2d and 3d). Furthermore, the magnitude of frequency decreases observed with protein/inhibitor complexes was higher than those observed with the apo proteins. Together, these data clearly indicate that the binding of clorgyline and rasagiline altered the interaction of MAO-A and MOA-B, respectively, with the negatively charged, DOPS-containing bilayer. We note that these differences in the net frequency changes could still be observed after taking into account possible contributions from free inhibitor molecules at respective concentrations (Figure S8a,b), thus ruling out the possibility that these differences are due to the binding of free inhibitor molecules. These differences in the binding of the apo and holo proteins further indicate that the proteins used in the study are present in their native, functional states. It is possible that the binding of inhibitors results in a conformational change in the proteins, which enables the increased binding of the proteins to the bilayers. However, structural alignment of the rasagiline free (PDB ID 1GOS)[24] and rasagiline bound (PDB ID 2BK4)[25] structures of MAO-B does not show either a change in the surface charge distribution (Figure S4a,b) or a change in the overall structure of the protein (root-mean-square difference in the C$\alpha$ atoms of 0.6 Å for all residues in the dimer) (Figure S4c). This suggests that the inhibitors are perhaps altering the structural dynamics of the proteins,[56−59] a feature that is not retained in the crystallized form of the proteins and is thus not observed in the structures determined by X-ray crystallography, leading to enhanced binding to the negatively charged bilayers.

The incubation of MAO-A/clorgyline and MAO-B/rasagiline complexes with the positively charged, DOEPC-containing bilayers (Figure 6d) did not result in any discernible change in the trend of either net frequency decreases (Figures S9b, S10b, and 6e,f) or net energy dissipations (Figurse S9c,d and S10c,d) when compared to the apo proteins. These data suggest that 30% DOEPC-containing bilayers possess a high binding capacity for the proteins, which makes the protein limiting under the concentrations tested here, and thus no discernible change could be seen in the trends with the protein/inhibitor complexes even if the inhibitors increased the binding of the proteins to the bilayers. Importantly, small but consistent differences in the energy dissipation could be observed between inhibitor-free and inhibitor-bound proteins in the intermediate frequency ranges (Figure S11a,b), indicating a difference in the viscoelastic properties of the protein-bound bilayers. This suggests that the binding of these inhibitors results in an increase in the structural dynamics of the proteins, which perhaps explains the increased binding of MAO-A/clorgyline and MAO-B/rasagiline to the negatively charged bilayers.

## ■ CONCLUSIONS

We have studied the interaction of MAO-A and MAO-B with phospholipid membranes in real time by combining the SLB format and QCM-D. On the basis of the data presented here, it is clear that the surface charge dictates the binding of the proteins to membranes (Figure 7). We propose that the membrane binding of MAO-A and MAO-B is a two-step process comprising (i) an initial transient interaction of the proteins with phospholipid headgroups and (ii) a stable insertion of the protein into the phospholipid membranes. While the initial interaction is possible with the zwitterionic, neutral DOPC bilayers, the stable insertion of the proteins requires the availability of charged lipid molecules. Furthermore, individual MAO-A and MAO-B protein molecules engage multiple negatively charged lipid molecules but fewer positively charged lipid molecules. However, the irreversible binding of MAO-A and MAO-B to clorgyline and rasagiline, respectively, decreases the number of negatively charged lipid molecules required for their stable insertion into the bilayers.

The experiments presented here were directed toward the reconstitution of MAO-A and MAO-B in an in vitro, supported lipid bilayer-based platform. However, the mitochondrial membrane surface charge has been shown to alter the protein binding,[60] thus we have varied the composition of the bilayers from negatively to neutral to positive. With the experimental setup reported here, we intend to work with more sophisticated platforms mimicking mitochondrial membranes in the future. It it important to realize that the assembly of supported lipid bilayers is affected by a variety of factors including lipid composition and charge[61−81] and that the development of


DOI: 10.1021/acs.langmuir.8b01348
Langmuir 2018, 34, 10764−10773

mitochondrial outer membrane-mimicking supported lipid bilayers will require a systematic evaluation and adjustment of different parameters. In summary, the results presented here not only provide insight into the mechanism of membrane binding of MOA-A and MAO-B but also will be instrumental in designing physiologically relevant experiments including the determination of their lipid preference and the screening of novel pharmacological agents.

## ■ ASSOCIATED CONTENT

### Supporting Information

The Supporting Information is available free of charge on the ACS Publications website at DOI: 10.1021/acs.langmuir.8b01348.

Descriptions of lipid structure, SDS-PAGE analysis, additional QCM-D analysis, protein structural analysis, and inhibitor-enzyme characterization (PDF)

## ■ AUTHOR INFORMATION


### Corresponding Authors

*E-mail: iamlli@njtech.edu.cn.
*E-mail: njcho@ntu.edu.sg.

### ORCID

Kabir H. Biswas: 0000-0001-9194-4127
Jay T. Groves: 0000-0002-3037-5220
Nam-Joon Cho: 0000-0002-8692-8955


### Author Contributions

⊥These authors contributed equally.

### Notes

The authors declare no competing financial interest.

## ■ ACKNOWLEDGMENTS

This work was supported by the National Research Foundation of Singapore through a competitive research programme grant (NRF-CRP10-2012-07) and a proof-of-concept grant (NRF2015NRF-POC0001-19) as well as through the Centre for Precision Biology at Nanyang Technological University. This work was also financially supported by the National Natural Science Foundation of China (nos. 81672508 and 61505076) and the Jiangsu Provincial Foundation for Distinguished Young Scholars (BK20170041).

## ■ REFERENCES


(1) Ramsay, R. R. Monoamine Oxidases: The Biochemistry of the Proteins as Targets in Medicinal Chemistry and Drug Discovery. *Curr. Top. Med. Chem.* **2012**, *12* (20), 2189−2209.

(2) Chajkowski-Scarry, S.; Rimoldi, J. M. Monoamine Oxidase a and B Substrates: Probing the Pathway for Drug Development. *Future Med. Chem.* **2014**, *6* (6), 697−717.

(3) Edmondson, D. E. Hydrogen Peroxide Produced by Mitochondrial Monoamine Oxidase Catalysis: Biological Implications. *Curr. Pharm. Des.* **2014**, *20* (2), 155−60.

(4) Shih, J. C.; Chen, K.; Ridd, M. J. Monoamine Oxidase: From Genes to Behavior. *Annu. Rev. Neurosci.* **1999**, *22*, 197−217.

(5) Wang, C. C.; Billett, E.; Borchert, A.; Kuhn, H.; Ufer, C. Monoamine Oxidases in Development. *Cell. Mol. Life Sci.* **2013**, *70* (4), 599−630.

(6) Brunner, H. G.; Nelen, M.; Breakefield, X. O.; Ropers, H. H.; van Oost, B. A. Abnormal Behavior Associated with a Point Mutation in the Structural Gene for Monoamine Oxidase A. *Science* **1993**, *262* (5133), 578−80.

(7) Brunner, H. G.; Nelen, M. R.; van Zandvoort, P.; Abeling, N. G.; van Gennip, A. H.; Wolters, E. C.; Kuiper, M. A.; Ropers, H. H.; van Oost, B. A. X-Linked Borderline Mental Retardation with Prominent Behavioral Disturbance: Phenotype, Genetic Localization, and Evidence for Disturbed Monoamine Metabolism. *Am. J. Hum. Genet.* **1993**, *52* (6), 1032−9.

(8) Piton, A.; Poquet, H.; Redin, C.; Masurel, A.; Lauer, J.; Muller, J.; Thevenon, J.; Herenger, Y.; Chancenotte, S.; Bonnet, M.; Pinoit, J. M.; Huet, F.; Thauvin-Robinet, C.; Jaeger, A. S.; Le Gras, S.; Jost, B.; Gerard, B.; Peoc'h, K.; Launay, J. M.; Faivre, L.; Mandel, J. L. 20 Ans Apres: A Second Mutation in Maoa Identified by Targeted High-Throughput Sequencing in a Family with Altered Behavior and Cognition. *Eur. J. Hum. Genet.* **2014**, *22* (6), 776−83.

(9) McDermott, R.; Tingley, D.; Cowden, J.; Frazzetto, G.; Johnson, D. D. Monoamine Oxidase a Gene (Maoa) Predicts Behavioral Aggression Following Provocation. *Proc. Natl. Acad. Sci. U. S. A.* **2009**, *106* (7), 2118−23.

(10) Lenders, J. W.; Eisenhofer, G.; Abeling, N. G.; Berger, W.; Murphy, D. L.; Konings, C. H.; Wagemakers, L. M.; Kopin, I. J.; Karoum, F.; van Gennip, A. H.; Brunner, H. G. Specific Genetic Deficiencies of the a and B Isoenzymes of Monoamine Oxidase Are Characterized by Distinct Neurochemical and Clinical Phenotypes. *J. Clin. Invest.* **1996**, *97* (4), 1010−9.

(11) Collins, F. A.; Murphy, D. L.; Reiss, A. L.; Sims, K. B.; Lewis, J. G.; Freund, L.; Karoum, F.; Zhu, D.; Maumenee, I. H.; Antonarakis, S. E. Clinical, Biochemical, and Neuropsychiatric Evaluation of a Patient with a Contiguous Gene Syndrome Due to a Microdeletion Xp11.3 Including the Norrie Disease Locus and Monoamine Oxidase (Maoa and Maob) Genes. *Am. J. Med. Genet.* **1992**, *42* (1), 127−34.

(12) Bortolato, M.; Chen, K.; Shih, J. C. Monoamine Oxidase Inactivation: From Pathophysiology to Therapeutics. *Adv. Drug Delivery Rev.* **2008**, *60* (13−14), 1527−33.

(13) Delumeau, J. C.; Bentue-Ferrer, D.; Gandon, J. M.; Amrein, R.; Belliard, S.; Allain, H. Monoamine Oxidase Inhibitors, Cognitive Functions and Neurodegenerative Diseases. *J. Neural Transm., Suppl.* **1994**, *41*, 259−66.

(14) Deshwal, S.; Di Sante, M.; Di Lisa, F.; Kaludercic, N. Emerging Role of Monoamine Oxidase as a Therapeutic Target for Cardiovascular Disease. *Curr. Opin. Pharmacol.* **2017**, *33*, 64−69.

(15) Li, P. C.; Siddiqi, I. N.; Mottok, A.; Loo, E. Y.; Wu, C. H.; Cozen, W.; Steidl, C.; Shih, J. C. Monoamine Oxidase a Is Highly Expressed in Classical Hodgkin Lymphoma. *J. Pathol.* **2017**, *243* (2), 220−229.

(16) Wu, J. B.; Shao, C.; Li, X.; Li, Q.; Hu, P.; Shi, C.; Li, Y.; Chen, Y. T.; Yin, F.; Liao, C. P.; Stiles, B. L.; Zhau, H. E.; Shih, J. C.; Chung, L. W. Monoamine Oxidase a Mediates Prostate Tumorigenesis and Cancer Metastasis. *J. Clin. Invest.* **2014**, *124* (7), 2891−908.

(17) Cai, Z. Monoamine Oxidase Inhibitors: Promising Therapeutic Agents for Alzheimer's Disease (Review). *Mol. Med. Rep.* **2014**, *9* (5), 1533−41.

(18) Binda, C.; Milczek, E. M.; Bonivento, D.; Wang, J.; Mattevi, A.; Edmondson, D. E. Lights and Shadows on Monoamine Oxidase Inhibition in Neuroprotective Pharmacological Therapies. *Curr. Top. Med. Chem.* **2011**, *11* (22), 2788−2796.

(19) Youdim, M. B.; Edmondson, D.; Tipton, K. F. The Therapeutic Potential of Monoamine Oxidase Inhibitors. *Nat. Rev. Neurosci.* **2006**, *7* (4), 295−309.

(20) Li, L.; Zhang, C. W.; Chen, G. Y.; Zhu, B.; Chai, C.; Xu, Q. H.; Tan, E. K.; Zhu, Q.; Lim, K. L.; Yao, S. Q. A Sensitive Two-Photon Probe to Selectively Detect Monoamine Oxidase B Activity in Parkinson's Disease Models. *Nat. Commun.* **2014**, *5*, 3276.

(21) Ghislieri, D.; Houghton, D.; Green, A. P.; Willies, S. C.; Turner, N. J. Monoamine Oxidase (Mao-N) Catalyzed Deracemization of Tetrahydro-B-Carbolines: Substrate Dependent Switch in Enantioselectivity. *ACS Catal.* **2013**, *3* (12), 2869−2872.

(22) Huang, R. H. Lipid-Protein Interactions in the Multiple Forms of Monoamine Oxidase. Enzymatic and Esr Studies with Purified Intact Rat Brain Mitochondria. *Mol. Pharmacol.* **1980**, *17* (2), 192−198.

(23) Navarro-Welch, C.; McCauley, R. B. An Evaluation of Phospholipids as Regulators of Monoamine Oxidase a and Mono-




DOI: 10.1021/acs.langmuir.8b01348
*Langmuir* 2018, 34, 10764−10773

amine Oxidase B Activities. *J. Biol. Chem.* **1982**, *257* (22), 13645−13649.
(24) Binda, C.; Newton-Vinson, P.; Hubalek, F.; Edmondson, D. E.; Mattevi, A. Structure of Human Monoamine Oxidase B, a Drug Target for the Treatment of Neurological Disorders. *Nat. Struct. Biol.* **2002**, *9* (1), 22−6.
(25) Hubalek, F.; Binda, C.; Khalil, A.; Li, M.; Mattevi, A.; Castagnoli, N.; Edmondson, D. E. Demonstration of Isoleucine 199 as a Structural Determinant for the Selective Inhibition of Human Monoamine Oxidase B by Specific Reversible Inhibitors. *J. Biol. Chem.* **2005**, *280* (16), 15761−6.
(26) De Colibus, L.; Li, M.; Binda, C.; Lustig, A.; Edmondson, D. E.; Mattevi, A. Three-Dimensional Structure of Human Monoamine Oxidase a (Mao a): Relation to the Structures of Rat Mao a and Human Mao B. *Proc. Natl. Acad. Sci. U. S. A.* **2005**, *102* (36), 12684−9.
(27) Son, S. Y.; Ma, J.; Kondou, Y.; Yoshimura, M.; Yamashita, E.; Tsukihara, T. Structure of Human Monoamine Oxidase a at 2.2-a Resolution: The Control of Opening the Entry for Substrates/Inhibitors. *Proc. Natl. Acad. Sci. U. S. A.* **2008**, *105* (15), 5739−44.
(28) Chen, K.; Wu, H. F.; Shih, J. C. Influence of C Terminus on Monoamine Oxidase a and B Catalytic Activity. *J. Neurochem.* **1996**, *66* (2), 797−803.
(29) Rebrin, I.; Geha, R. M.; Chen, K.; Shih, J. C. Effects of Carboxyl-Terminal Truncations on the Activity and Solubility of Human Monoamine Oxidase B. *J. Biol. Chem.* **2001**, *276* (31), 29499−506.
(30) Binda, C.; Newton-Vinson, P.; Hubalek, F.; Edmondson, D. E.; Mattevi, A. Structure of Human Monoamine Oxidase B, a Drug Target for the Treatment of Neurological Disorders. *Nat. Struct. Biol.* **2002**, *9* (1), 22−6.
(31) Fowler, P. W.; Balali-Mood, K.; Deol, S.; Coveney, P. V.; Sansom, M. S. P. Monotopic Enzymes and Lipid Bilayers: A Comparative Study. *Biochemistry* **2007**, *46*, 3108−3115.
(32) Huang, R. H.; Faulkner, R. The Role of Phospholipid in the Multiple Functional Forms of Brain Monoamine Oxidase. *J. Biol. Chem.* **1981**, *256* (17), 9211−9215.
(33) Zhuang, Z. P.; Marks, B.; McCauley, R. B. The Insertion of Monoamine Oxidase a into the Outer Membrane of Rat Liver Mitochondria. *J. Biol. Chem.* **1992**, *267* (1), 591−596.
(34) Zhuang, Z.; Hogan, M.; McCauley, R. The in Vitro Insertion of Monoamine Oxidase B into Mitochondrial Outer Membranes. *FEBS Lett.* **1988**, *238* (1), 185−90.
(35) Zhaung, Z. P.; McCauley, R. Ubiquitin Is Involved in the in Vitro Insertion of Monoamine Oxidase B into Mitochondrial Outer Membranes. *J. Biol. Chem.* **1989**, *264* (25), 14594−14596.
(36) Cruz, F.; Edmondson, D. E. Kinetic Properties of Recombinant Mao-a on Incorporation into Phospholipid Nanodisks. *J. Neural. Transm. (Vienna)* **2007**, *114* (6), 699−702.
(37) Cho, N. J.; Frank, C. W.; Kasemo, B.; Hook, F. Quartz Crystal Microbalance with Dissipation Monitoring of Supported Lipid Bilayers on Various Substrates. *Nat. Protoc.* **2010**, *5* (6), 1096−106.
(38) Rodahl, M.; Hook, F.; Fredriksson, C.; Keller, C. A.; Krozer, A.; Brzezinski, P.; Voinova, M.; Kasemo, B. Simultaneous Frequency and Dissipation Factor Qcm Measurements of Biomolecular Adsorption and Cell Adhesion. *Faraday Discuss.* **1997**, *107*, 229−46.
(39) Keller, C. A.; Kasemo, B. Surface Specific Kinetics of Lipid Vesicle Adsorption Measured with a Quartz Crystal Microbalance. *Biophys. J.* **1998**, *75* (3), 1397−1402.
(40) Tabaei, S. R.; Choi, J. H.; Haw Zan, G.; Zhdanov, V. P.; Cho, N. J. Solvent-Assisted Lipid Bilayer Formation on Silicon Dioxide and Gold. *Langmuir* **2014**, *30* (34), 10363−73.
(41) Rodahl, M.; Höök, F.; Krozer, A.; Brzezinski, P.; Kasemo, B. Quartz Crystal Microbalance Setup for Frequency and Q-Factor Measurements in Gaseous and Liquid Environments. *Rev. Sci. Instrum.* **1995**, *66* (7), 3924−3930.
(42) Cho, N. J.; Jackman, J. A.; Liu, M.; Frank, C. W. Ph-Driven Assembly of Various Supported Lipid Platforms: A Comparative Study on Silicon Oxide and Titanium Oxide. *Langmuir* **2011**, *27* (7), 3739−48.
(43) Tabaei, S. R.; Vafaei, S.; Cho, N. J. Fabrication of Charged Membranes by the Solvent-Assisted Lipid Bilayer (Salb) Formation Method on $SiO_2$ and $Al_2O_3$. *Phys. Chem. Chem. Phys.* **2015**, *17* (17), 11546−52.
(44) Vafaei, S.; Tabaei, S. R.; Biswas, K. H.; Groves, J. T.; Cho, N.-J. Dynamic Cellular Interactions with Extracellular Matrix Triggered by Biomechanical Tuning of Low-Rigidity, Supported Lipid Membranes. *Adv. Healthcare Mater.* **2017**, *6* (10), 1700243.
(45) Novaroli, L.; Reist, M.; Favre, E.; Carotti, A.; Catto, M.; Carrupt, P. A. Human Recombinant Monoamine Oxidase B as Reliable and Efficient Enzyme Source for Inhibitor Screening. *Bioorg. Med. Chem.* **2005**, *13* (22), 6212−7.
(46) Rojas, R. J.; Edmondson, D. E.; Almos, T.; Scott, R.; Massari, M. E. Reversible and Irreversible Small Molecule Inhibitors of Monoamine Oxidase B (Mao-B) Investigated by Biophysical Techniques. *Bioorg. Med. Chem.* **2015**, *23* (4), 770−8.
(47) Milczek, E. M.; Binda, C.; Rovida, S.; Mattevi, A.; Edmondson, D. E. The 'Gating' Residues Ile199 and Tyr326 in Human Monoamine Oxidase B Function in Substrate and Inhibitor Recognition. *FEBS J.* **2011**, *278* (24), 4860−9.
(48) Lee, A. G. How Lipids and Proteins Interact in a Membrane: A Molecular Approach. *Mol. BioSyst.* **2005**, *1* (3), 203−12.
(49) Jackman, J. A.; Cho, N. J.; Duran, R. S.; Frank, C. W. Interfacial Binding Dynamics of Bee Venom Phospholipase A2 Investigated by Dynamic Light Scattering and Quartz Crystal Microbalance. *Langmuir* **2010**, *26* (6), 4103−12.
(50) Binda, C.; Hubalek, F.; Li, M.; Edmondson, D. E.; Mattevi, A. Crystal Structure of Human Monoamine Oxidase B, a Drug Target Enzyme Monotopically Inserted into the Mitochondrial Outer Membrane. *FEBS Lett.* **2004**, *564* (3), 225−8.
(51) Famulski, K. S.; Nalecz, M. J.; Wojtczak, L. Phosphorylation of Mitochondrial Membrane Proteins: Effect of the Surface Potential on Monoamine Oxidase. *FEBS Lett.* **1983**, *157* (1), 124−8.
(52) Cao, X.; Rui, L.; Pennington, P. R.; Chlan-Fourney, J.; Jiang, Z.; Wei, Z.; Li, X. M.; Edmondson, D. E.; Mousseau, D. D. Serine 209 Resides within a Putative P38(Mapk) Consensus Motif and Regulates Monoamine Oxidase-a Activity. *J. Neurochem.* **2009**, *111* (1), 101−10.
(53) Wang, J.; Harris, J.; Mousseau, D. D.; Edmondson, D. E. Mutagenic Probes of the Role of Ser209 on the Cavity Shaping Loop of Human Monoamine Oxidase A. *FEBS J.* **2009**, *276* (16), 4569−81.
(54) Geha, R. M.; Rebrin, I.; Chen, K.; Shih, J. C. Substrate and Inhibitor Specificities for Human Monoamine Oxidase a and B Are Influenced by a Single Amino Acid. *J. Biol. Chem.* **2001**, *276* (13), 9877−82.
(55) Youdim, M. B.; Gross, A.; Finberg, J. P. Rasagiline [N-Propargyl-1r(+)-Aminoindan], a Selective and Potent Inhibitor of Mitochondrial Monoamine Oxidase B. *Br. J. Pharmacol.* **2001**, *132* (2), 500−6.
(56) Popovych, N.; Sun, S.; Ebright, R. H.; Kalodimos, C. G. Dynamically Driven Protein Allostery. *Nat. Struct. Mol. Biol.* **2006**, *13* (9), 831−8.
(57) Biswas, K. H.; Visweswariah, S. S. Distinct Allostery Induced in the Cyclic Gmp-Binding, Cyclic Gmp-Specific Phosphodiesterase (Pde5) by Cyclic Gmp, Sildenafil, and Metal Ions. *J. Biol. Chem.* **2011**, *286* (10), 8545−54.
(58) Biswas, K. H.; Badireddy, S.; Rajendran, A.; Anand, G. S.; Visweswariah, S. S. Cyclic Nucleotide Binding and Structural Changes in the Isolated Gaf Domain of Anabaena Adenylyl Cyclase, Cyab2. *PeerJ* **2015**, *3*, e882.
(59) Kim, T. H.; Mehrabi, P.; Ren, Z.; Sljoka, A.; Ing, C.; Bezginov, A.; Ye, L.; Pomes, R.; Prosser, R. S.; Pai, E. F. The Role of Dimer Asymmetry and Protomer Dynamics in Enzyme Catalysis. *Science* **2017**, *355* (6322), eaag2355.
(60) Heit, B.; Yeung, T.; Grinstein, S. Changes in Mitochondrial Surface Charge Mediate Recruitment of Signaling Molecules During Apoptosis. *American journal of physiology. Cell physiology* **2011**, *300* (1), C33−41.


DOI: 10.1021/acs.langmuir.8b01348
*Langmuir* 2018, 34, 10764−10773

(61) Biswas, K. H.; Jackman, J. A.; Park, J. H.; Groves, J. T.; Cho, N. J. Interfacial Forces Dictate the Pathway of Phospholipid Vesicle Adsorption onto Silicon Dioxide Surfaces. *Langmuir* **2018**, *34* (4), 1775−1782.
(62) Cremer, P. S.; Boxer, S. G. Formation and Spreading of Lipid Bilayers on Planar Glass Supports. *J. Phys. Chem. B* **1999**, *103* (13), 2554−2559.
(63) Dimitrievski, K.; Kasemo, B. Influence of Lipid Vesicle Composition and Surface Charge Density on Vesicle Adsorption Events: A Kinetic Phase Diagram. *Langmuir* **2009**, *25* (16), 8865−8869.
(64) Reviakine, I.; Gallego, M.; Johannsmann, D.; Tellechea, E. Adsorbed Liposome Deformation Studied with Quartz Crystal Microbalance. *J. Chem. Phys.* **2012**, *136* (8), 084702.
(65) Jackman, J. A.; Choi, J.-H.; Zhdanov, V. P.; Cho, N.-J. Influence of Osmotic Pressure on Adhesion of Lipid Vesicles to Solid Supports. *Langmuir* **2013**, *29* (36), 11375−11384.
(66) Reimhult, E.; Höök, F.; Kasemo, B. Intact Vesicle Adsorption and Supported Biomembrane Formation from Vesicles in Solution: Influence of Surface Chemistry, Vesicle Size, Temperature, and Osmotic Pressure. *Langmuir* **2003**, *19* (5), 1681−1691.
(67) Boudard, S.; Seantier, B.; Breffa, C.; Decher, G.; Félix, O. Controlling the Pathway of Formation of Supported Lipid Bilayers of Dmpc by Varying the Sodium Chloride Concentration. *Thin Solid Films* **2006**, *495* (1), 246−251.
(68) Seantier, B.; Breffa, C.; Felix, O.; Decher, G. Dissipation-Enhanced Quartz Crystal Microbalance Studies on the Experimental Parameters Controlling the Formation of Supported Lipid Bilayers. *J. Phys. Chem. B* **2005**, *109* (46), 21755−65.
(69) Johnson, J. M.; Ha, T.; Chu, S.; Boxer, S. G. Early Steps of Supported Bilayer Formation Probed by Single Vesicle Fluorescence Assays. *Biophys. J.* **2002**, *83* (6), 3371−9.
(70) Gozen, I.; Jesorka, A. Instrumental Methods to Characterize Molecular Phospholipid Films on Solid Supports. *Anal. Chem.* **2012**, *84* (2), 822−38.
(71) Mashaghi, A.; Mashaghi, S.; Reviakine, I.; Heeren, R. M.; Sandoghdar, V.; Bonn, M. Label-Free Characterization of Biomembranes: From Structure to Dynamics. *Chem. Soc. Rev.* **2014**, *43* (3), 887−900.
(72) Tero, R.; Ujihara, T.; Urisu, T. Lipid Bilayer Membrane with Atomic Step Structure: Supported Bilayer on a Step-and-Terrace Tio2(100) Surface. *Langmuir* **2008**, *24* (20), 11567−76.
(73) Cha, T.; Guo, A.; Zhu, X. Y. Formation of Supported Phospholipid Bilayers on Molecular Surfaces: Role of Surface Charge Density and Electrostatic Interaction. *Biophys. J.* **2006**, *90* (4), 1270−4.
(74) Tero, R.; Watanabe, H.; Urisu, T. Supported Phospholipid Bilayer Formation on Hydrophilicity-Controlled Silicon Dioxide Surfaces. *Phys. Chem. Chem. Phys.* **2006**, *8* (33), 3885−94.
(75) Jackman, J. A.; Zan, G. H.; Zhao, Z.; Cho, N. J. Contribution of the Hydration Force to Vesicle Adhesion on Titanium Oxide. *Langmuir* **2014**, *30* (19), 5368−72.
(76) Schonherr, H.; Johnson, J. M.; Lenz, P.; Frank, C. W.; Boxer, S. G. Vesicle Adsorption and Lipid Bilayer Formation on Glass Studied by Atomic Force Microscopy. *Langmuir* **2004**, *20* (26), 11600−6.
(77) Keller, C. A.; Glasmastar, K.; Zhdanov, V. P.; Kasemo, B. Formation of Supported Membranes from Vesicles. *Phys. Rev. Lett.* **2000**, *84* (23), 5443−6.
(78) Zhdanov, V. P.; Keller, C. A.; Glasmästar, K.; Kasemo, B. Simulation of Adsorption Kinetics of Lipid Vesicles. *J. Chem. Phys.* **2000**, *112* (2), 900−909.
(79) Zhdanov, V. P.; Kasemo, B. Comments on Rupture of Adsorbed Vesicles. *Langmuir* **2001**, *17* (12), 3518−3521.
(80) Seantier, B.; Kasemo, B. Influence of Mono-and Divalent Ions on the Formation of Supported Phospholipid Bilayers Via Vesicle Adsorption. *Langmuir* **2009**, *25* (10), 5767−5772.
(81) Mager, M. D.; Almquist, B.; Melosh, N. A. Formation and Characterization of Fluid Lipid Bilayers on Alumina. *Langmuir* **2008**, *24* (22), 12734−12737.



DOI: 10.1021/acs.langmuir.8b01348
*Langmuir* 2018, 34, 10764−10773